

Vortices in a Bose-Einstein condensate confined by an optical lattice

P.G. Kevrekidis[†], R. Carretero-González[‡], G. Theocharis[§],
D.J. Frantzeskakis[§], and B.A. Malomed^{||}

Abstract. We investigate the dynamics of vortices in repulsive Bose-Einstein condensates in the presence of an optical lattice (OL) and a parabolic magnetic trap. The dynamics is sensitive to the phase of the OL potential relative to the magnetic trap, and depends less on the OL strength. For the cosinusoidal OL potential, a local minimum is generated at the trap's center, creating a stable equilibrium for the vortex, while in the case of the sinusoidal potential, the vortex is expelled from the center, demonstrating spiral motion. Cases where the vortex is created far from the trap's center are also studied, revealing slow outward-spiraling drift. Numerical results are explained in an analytical form by means of a variational approximation. Finally, motivated by a discrete model (which is tantamount to the case of the strong OL lattice), we present a novel type of vortex consisting of two pairs of anti-phase solitons.

[†] Department of Mathematics and Statistics, University of Massachusetts, Amherst MA 01003-4515, USA

[‡] Nonlinear Dynamical Systems Group[¶], Department of Mathematics and Statistics, San Diego State University, San Diego CA, 92182-7720

[§] Department of Physics, University of Athens, Panepistimiopolis, Zografos, Athens 15784, Greece

^{||} Department of Interdisciplinary Studies, Faculty of Engineering, Tel Aviv University, Tel Aviv 69978, Israel

J. Phys. B: At. Mol. Phys. **36** (2003) 3467–3476.

The experimental realization and theoretical studies of Bose-Einstein condensates (BECs) [1] have led to an explosion of interest in the field of atomic matter waves and their nonlinear excitations, including dark [2] and bright [3] solitons. More recently, two-dimensional (2D) excitations, such as vortices [4] and vortex lattices [5], were considered and realized experimentally. Other nonlinear states, such as e.g., Faraday waves [6], ring dark solitons and vortex necklaces [7], stable solitons and localized vortices in attractive BECs trapped in a 2D optical lattice (OL) [8], and even stable solitons supported by an OL in a *repulsive* BEC [9] were also predicted.

Vortices, in particular, are worth studying not only due to their significance as a fundamental type of coherent nonlinear excitations, but also because they play a dominant role in the breakdown of superflow in Bose fluids [10, 11]. The theoretical description of vortices in BECs can be carried out in a much more efficient way than in liquid He [12] due to the weakness of interactions in the former case (which, in addition, is tunable [13]). These advantages explain a large volume of work regarding the behavior of vortices in BECs, which has been recently summarized in a review [14].

The subject of the present paper is the dynamics of vortices under the action of the OL; to the best of our knowledge, this problem is considered in this work for the first time. An OL potential is generated as an interference pattern by laser beams illuminating the condensate, in particular in 1D and 2D cases [15, 16, 17, 18, 19]. In the 2D case, the OL potential assumes the form (in dimensionless units)

$$V_{\text{OL}}(x, y) = V_0 [\cos^2(kx + \phi) + \cos^2(ky + \phi)], \quad (1)$$

where V_0 is the strength of the OL, which is measured in units of the recoil energy $E_r = \hbar^2/2m\lambda_{\text{laser}}^2$ (i.e., the kinetic energy gained by an atom when it absorbs a photon from the OL), where λ_{laser} is the laser wavelength, \hbar is Planck's constant, m is the atomic mass, k is the wavenumber of the OL, and ϕ is a phase-detuning factor [the obvious possibility to remove ϕ by means of the diagonal shift, $(x, y) \rightarrow (x - \phi/k, y - \phi/k)$, is ruled out by the presence of the magnetic-trap potential, see below]. The wavenumber k of the OL can be experimentally controlled by varying the angle between the counter-propagating lasers producing the interference pattern [20].

As is well known, the effective 2D GP equation applies to situations when the condensate has a nearly planar (“pancake”) shape, see, e.g., [21] and references therein. Accordingly, vortex states considered below are not subject to 3D instabilities (corrugation of the vortex axis [14]) as the transverse dimension is effectively suppressed. We base the analysis on the Gross-Pitaevskii (GP) equation, written in harmonic-oscillator units [22],

$$iu_t = -\Delta u + |u|^2 u + V(x, y) u, \quad (2)$$

where $u = u(x, y, t)$ is the 2D wave function, and the external potential is

$$V(x, y) = \frac{1}{2}\Omega^2(x^2 + y^2) + V_{\text{OL}}(x, y), \quad (3)$$

which includes the isotropic magnetic trap [1] and OL potential (1). Notice that the dimensionless parameter $\Omega \equiv \omega_r/\omega_z$ in Eq. (3), where $\omega_{r,z}$ are the confinement frequencies in the radial and axial directions respectively, is assumed to be $\Omega \ll 1$. In most studies of vortices, angular momentum imparted by stirring of the condensate is assumed (see, e.g., [23, 24] and references therein), as typically this is the way in which vortices are generated in experimental settings [4]. Here we assume that a vortex has been generated, but then the stirring ceases. Alternatively, the vortex may be created

by means of the phase-engineering technique [25]. The positive sign in front of the nonlinear term in Eq. (2) implies that we consider a repulsive condensate.

We first present numerical findings for the case of a “regular” vortex; subsequently, the observed dynamics is explained by means of a variational approximation. We then proceed to examine a new type of a vortex, which is a robust bound state of two pairs of π -out-of-phase pulses, as suggested by results known for 2D dynamical lattices. In most cases, we fix the strength of the magnetic-trap potential to be $\Omega^2 = 0.002$. This value is relevant to a ^{87}Rb condensate of radius $25\mu\text{m}$, containing 4.6×10^4 atoms in a highly anisotropic trap with $\omega_r = 2\pi \times 7.5$ Hz and $\omega_z = 2\pi \times 115$ Hz. According to these values of the physical parameters, in the following results, which will be presented in normalized time and space units, the corresponding units are 1.38 ms and $1\mu\text{m}$ respectively. Additionally, as far as the OL parameters are concerned, the typical values $V_0 = 0.5$ and $k = 1$ used in most cases, correspond to $0.5E_r$ and to an OL wavelength of $6.3\mu\text{m}$.

In simulations, the initial vortex configuration is taken, in polar coordinates ρ and θ , as

$$u = \rho(r) \exp(i\theta) u_{\text{TF}}, \quad (4)$$

where $\rho(r) = r^2(0.34 + 0.07r^2)/(1 + 0.41r^2 + 0.07r^4)$ is the radial Padé interpolation for the vortex solution to the GP equation without external potential, and $u_{\text{TF}} = \sqrt{\max\{0, \mu - (\Omega^2/2)(x^2 + y^2)\}}$ is the Thomas-Fermi (TF) wave function for the magnetic trap [1], with a chemical potential μ . The vortex is placed at the center of the magnetic trap (unless otherwise indicated). Simulations were performed by means of a finite-difference discretization in a box of the size 60×60 ($60\mu\text{m} \times 60\mu\text{m}$), using 200×200 points (i.e., the spatial stepsizes are $dx = dy = 0.3$). Time integration was performed by means of the fourth-order Runge-Kutta scheme with the time step $dt = 0.0025$ ($dt = 3.45\mu\text{s}$). It should be remarked that in the initial stages of the time evolution, the initial condition of Eq. (4) “adjusts” itself to the presence of the OL, by shedding small amplitude radiation waves. These are dissipated by the an absorbing region close to the boundary implemented in the numerical simulation.

The first case that was examined is the one with $\phi = 0$ in Eq. (1). In this case, the vortex is extremely robust, staying at the center during a few hundred time units of Eq. (2), which correspond to a few hundred of milliseconds in physical units. As can be seen in Fig. 1, where the vortex and its motion are shown for $V_0 = 0.5$ and $k = 1$, the displacement of the vortex center remains, indefinitely long, as small as $\sim 10^{-3}$. The center of the vortex was located by fitting, close to the local minimum, the density $|u|^2$ to the expression $|u|^2 = Ax^2 + By^2 + Cx + Dy + E$, which yields the position of the center at $(-C/2A, -B/2D)$.

In Fig. 2, we display the evolution which starts from the same initial configuration, but with $\phi = \pi/2$ in Eq. (1). A distinctly different behavior is observed in this case, which is shown for longer times, up to $t = 250$ (346 ms), to verify that it is a real feature. In particular, it is clearly observed in this case that the vortex *spirals out* from the center of the magnetic trap. Note that fine details of the motion indicate meandering motion, similar to that exhibited by spiral waves in excitable media [26], even though in the present case the meandering occurs on a smaller spatial scale, hence much finer resolution would be needed to clarify it. However, the outward-spiraling motion of the vortex center is clearly seen in Fig. 2. Considerably longer runs [for times on the order of a few thousand time units of Eq. (2), which correspond to seconds in physical units] show that the vortex spirals all the way to the edges of

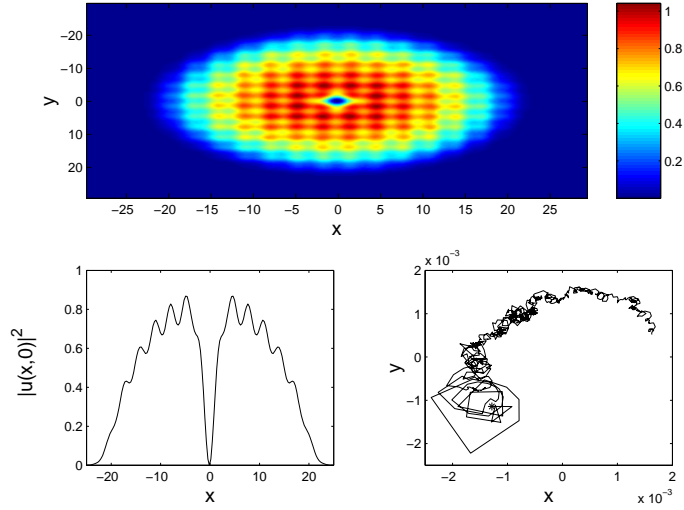


Figure 1. The vortex on a BEC of diameter $\approx 50\mu\text{m}$ in the cosinusoidal [$\phi = 0$ in Eq. (1)] OL potential with $V_0 = 0.5$ and $k = 1$. The top panel shows the contour plot of the density at $t = 100$ (138 ms). The bottom left panel is a cut of the same density profile along $x = 0$, while the bottom right one shows the motion of the vortex center for $0 \leq t \leq 100$, the initial position being marked by a star. Notice the scale (10^{-3} , or 1 nm in physical units) of very weak jiggling of the vortex, which thus stays practically immobile at the origin.

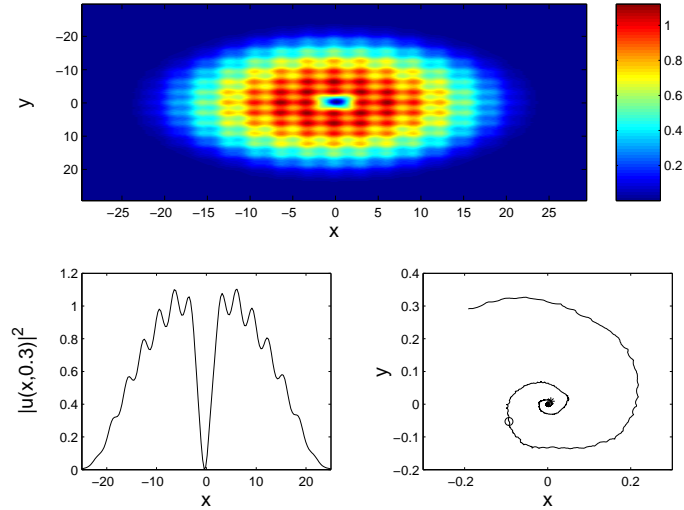


Figure 2. The same as in Fig. 1, but now the potential is sinusoidal, $\phi = \pi/2$. To clearly demonstrate the dynamics, the top and bottom left panels show the density profiles at a larger time than in Fig. 1, $t = 250$ (346 ms). The bottom right panel depicts the motion of the vortex center for $0 \leq t \leq 250$ [positions of the vortex center at $t = 100$ (138 ms) and $t = 200$ (276 ms), respectively, are indicated by the star and circle].

the TF cloud where it eventually decays (see also comments below).

In Fig. 3, we examine the case with $\phi = \pi/4$ in Eq. (1). In this case also, the

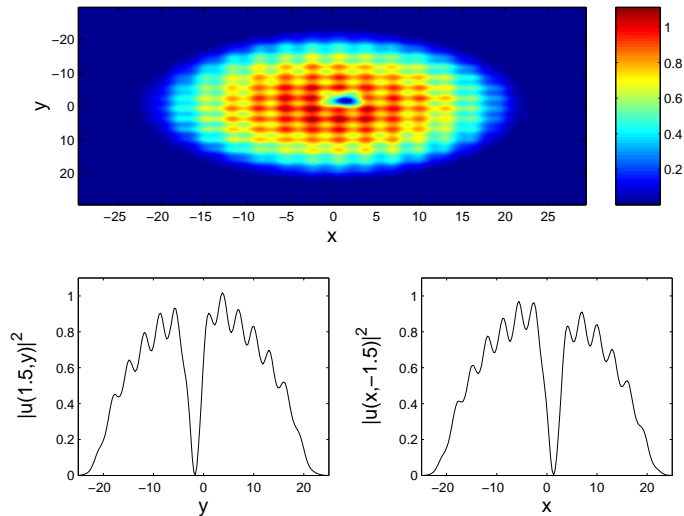


Figure 3. The case of $V_0 = 0.5$ and $\phi = \pi/4$ in Eq. (1). The vortex moves rapidly away from the center. The snapshots show the density profile (top panel) and its horizontal and vertical cuts (along $x = 1.5$ and $y = -1.5$, respectively) of the field at $t = 100$ (138 ms).

vortex moves outward. In fact, it is observed that it moves away from the trap center much faster, as at $t = 100$ (138 ms) it is already located near $(x, y) = (1.5, -1.5)$ (cf. Fig. 2), corresponding to a couple of μm from the trap center.

Qualitatively similar conclusions, but at different time scales, have been obtained for different values of the OL strength V_0 . For instance, in the potential with $\phi = \pi/2$, $V_0 = 1.5$ (and $k = 1$), the vortex spirals out again (similar to the case with $V_0 = 0.5$ displayed above), the time necessary for it to reach the distance of 0.1 from the origin being three times as large as in the case of $V_0 = 0.5$ (details are not shown here). This can be explained by the fact that, if V_0 is larger, the vortex has to move through a “rougher” energy landscape, hence it becomes more difficult for it to “find its way out”.

These findings can be qualitatively understood in terms of an effective potential which governs the motion of the vortex; in particular, the potential has a minimum and maximum at the center of the magnetic trap in the cases of $\phi = 0$ and $\phi = \pi/2$, respectively. To present this explanation in a mathematically tractable form, we resort to a variational approximation. As in Ref. [27], we use the following *ansatz* for the vortex, inspired by its linear analog namely the first excited state of the quantum harmonic oscillator:

$$u(x, y, t) = B(t) r_0(t) \exp[-r_0^2(t)/b(t)] e^{i\varphi_0(t)}, \quad (5)$$

where $r_0^2(t) \equiv (x - x_0(t))^2 + (y - y_0(t))^2$, and $\varphi_0(t) \equiv \tan^{-1}[(y - y_0(t))/(x - x_0(t))]$. Note that the *ansatz* carries a vortex-like structure centered at (x_0, y_0) , and it qualitatively emulates the initial waveform (4) which was adopted in the numerical simulations. The stronger the nonlinearity, the less accurate the approximation offered by Eq. (5) is; however, as the *ansatz* (5) was found to always provide a qualitatively correct description of the phenomenology, we use it to represent the vortex.

Similarly to the calculations reported in Refs. [28, 29], one can easily deduce

(additionally using the norm conservation) that the evolution of $B(t)$ and $b(t)$ is, to the leading order, negligible, therefore we set them to constant values, $B \approx B(t)$ and $b \approx b(t)$. Then, the substitution of the ansatz (5) into the Lagrangian of the GP equation (2) with the potential (3) leads, up to constant factors, to the effective Lagrangian

$$L = \frac{1}{2} (\dot{x}_0^2 + \dot{y}_0^2) - V_{\text{eff}}(x_0, y_0), \quad (6)$$

where the net effect of the OL and magnetic trap is combined into an effective potential,

$$V_{\text{eff}}(x, y) = Q(\phi) [\cos(2kx) + \cos(2ky)] + \frac{1}{4}\Omega^2 (x^2 + y^2), \quad (7)$$

where $Q(\phi)$ is given by a rather cumbersome expression; we will actually need the values

$$\begin{aligned} Q(0) &= \frac{V_0}{8} (bk^2 - 2) \exp(-bk^2/2), \\ Q\left(\frac{\pi}{2}\right) &= -Q(0), \quad \text{and} \\ Q\left(\frac{\pi}{4}\right) &= 0. \end{aligned}$$

Equations (6) and (7) suggest that the motion of the coordinates x_0 and y_0 of the vortex core resembles the motion of two uncoupled oscillators. Actually, this is a straightforward generalization of a result that can be obtained in the corresponding 1D case: in that case, the counterpart of the vortex is a dark soliton, whose equation of motion in the presence of the potential (3) can be derived by means of the adiabatic perturbation theory for dark solitons in BECs; see e.g., [30] and references therein. This approach, in the presence of the one-dimensional magnetic trap and OL, yields an effective potential

$$V_{\text{eff}}^{(1D)}(x) = \frac{1}{4}V_0 \left[1 - \frac{1}{6} \left(\frac{\pi^2}{3} - 2 \right) k^2 \right] \cos(2kx) + \frac{1}{4}\Omega^2 x^2.$$

In fact, Eq. (7) is a generalization of this expression. The effective potential from Eq. (7) is depicted in Fig. 4 as a function of x and y for the cases $\phi = 0$ and $\phi = \pi/2$, where we set $b = 1$ [this value was chosen, comparing the size of the numerically obtained vortex with that implied by the ansatz (5)].

In our experiments $k = 1$ was used, and thus, in the case $\phi = 0$, a vortex positioned at the center of the magnetic trap is at a local minimum of the potential (7), therefore the vortex stays in this position. If slightly perturbed around this stable fixed point, the vortex will perform small amplitude oscillations. On the contrary, in the case of $\phi = \pi/2$, the same point $(x_0, y_0) = (0, 0)$ is unstable (as a saddle), and as a result the vortex moves away from it. These conclusions are in full accord with the numerical experiments, see Figs. 1 and 2.

Normally, in a Hamiltonian mechanical system the motion from an unstable saddle point occurs along the corresponding unstable separatrix. However, it is well known [31, 32, 33] that a spatially-periodic setting may give rise to resonant effects, which induce an effective dissipation, due to emission of radiation waves from a nonlinear-wave state (vortex, in the present case). This effective dissipation, as is known [24, 34, 35, 36], causes the vortex to spiral outward (making the saddle point look like an unstable spiral), which is what we indeed observe in the simulations, see Fig.

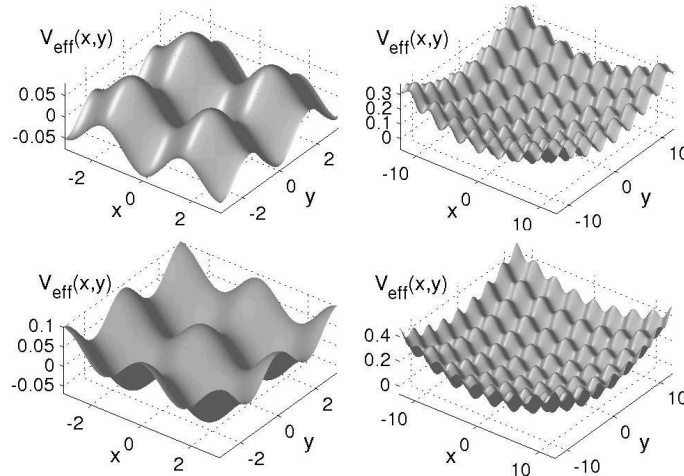


Figure 4. The effective potential $V_{\text{eff}}(x,y)$, obtained in the variational approximation [cf. Eq. (7)], responsible for the motion of the vortex subject to the 2D optical lattice and magnetic trap. Top panel: the cosinusoidal optical lattice ($\phi = 0$) produces a minimum in the effective potential at the origin. Bottom: the sinusoidal optical potential ($\phi = \pi/2$) gives rise to a maximum of the potential at the origin. The right panels display more clearly the combined effect of the optical lattice and magnetic trap (here we use $\Omega^2 = 0.005$, instead of $\Omega^2 = 0.002$, which was used in the computations). The parameters are $b = 1$, $k = 1$, $V_0 = 0.5$.

2. Note that in other cases where the Hamiltonian is not positive definite (such as e.g., Korteweg-de Vries – type models), radiative losses may destabilize an equilibrium position which is otherwise stable [37]. Finally, in the case of $\phi = \pi/4$, the center of the vortex is not originally at an equilibrium position of the potential of Eq. (1), hence its drift is manifested faster, as is indeed seen in Fig. 3.

Now we turn to a different case, in which the vortex was created far from the center of the magnetic trap (the results are displayed only for $\phi = 0$, as it was found that the value of ϕ does not significantly affect the results in this case). The motion of the vortex is displayed in Fig. 5, where its outward-spiraling, due to the effective dissipation induced by the optical lattice, is obvious. This spiral motion is combined with jiggling induced by the potential energy landscape. Thus, we conclude that a vortex seeded in the periphery of the BEC cloud will slowly drift towards the edge of the cloud, where it will eventually decay into other excitations [35].

Finally, we present a novel type of vortex, which is quite different from the one considered above. Motivated by recent investigations of vortices on 2D discrete lattices [38, 39], we initialized a real field configuration which is shown in the top panel of Fig. 6. The configuration consists of two up-down (dipolar) pulse pairs, each featuring a phase shift of π , hence a total phase shift along a contour surrounding these pulses is 2π , which corresponds to unit vorticity. In discrete lattices, numerically exact stable stationary solutions of this type exist [38]. In spatially uniform continuum models, such stationary solutions cannot exist, but Fig. 6 shows that they may be sustained by the OL. After shedding some radiation, the configuration reaches a nearly steady state, although residual oscillations are observed. Notice, once again, that waves radiated away due to the oscillations are absorbed by the dissipative boundaries of the integration domain (which were imposed to avoid artificial reflection). This

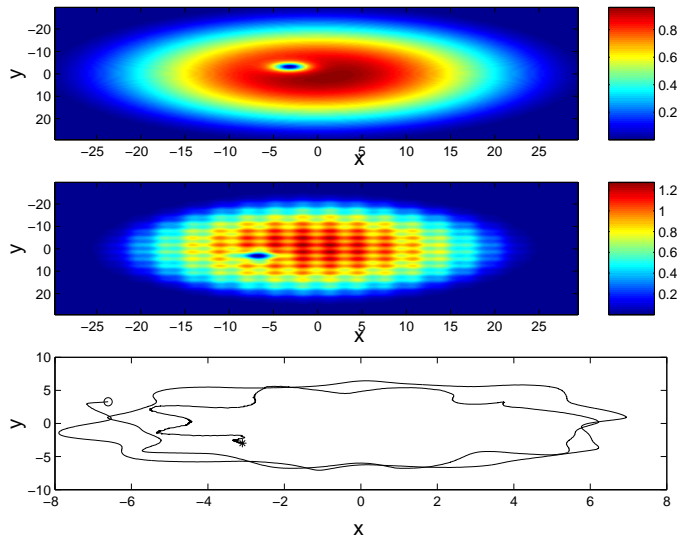


Figure 5. The top and middle panels show the vortex configuration at $t = 0$ and $t = 750$ (≈ 1 s). The bottom panel shows the trajectory of the vortex from $t = 0$ up to $t = 750$ (the two positions are marked by the star and circle, respectively).

dynamically stable, lattice-motivated configuration represents, to the best of our knowledge, a novel vortex-like structure which is particular to the system equipped with OL: without the lattice potential, the two π -out-of-phase sets of the in-phase pulses would separate due to the pulse-pulse interactions (which are repulsive in the case of opposite “parity” pulses and attractive in the case of same parity ones; see e.g., [40]). However, the effective potential exerts a “local force” on the pulses, making it possible to trap them together in a stable configuration of this type.

In conclusion, we have studied basic properties of vortices in the 2D Gross-Pitaevskii equation with the optical lattice (OL) and magnetic trap. The results crucially depend on the phase of the OL relative to the parabolic magnetic trap. Depending on the phase, it is possible to trap the vortex at the center of the trap, or, on the contrary, to expel it, which is readily explained in terms of an effective potential for the vortex derived by means of the variational approximation. In the latter case, the vortex moves along an unwinding spiral, which is explained by the effective dissipation due to emission of small-amplitude waves. We also considered the case in which the vortex was initially created far from the center of the trap, for which a precessing motion with a slow outward-spiraling drift was observed and qualitatively explained. Finally, a new species of a stable vortex, specific to the system equipped with the optical lattice, was found in the form of a bound state of two π -out-of-phase soliton pairs. The existence of this vortex is also explained by the OL-induced potential.

Naturally, it would be of interest to further examine structures which are inspired by features particular to periodically modulated models, and to observe how they appear and disappear with variation of the OL strength. Such studies are currently in progress.

This work was supported by a UMass FRG and NSF-DMS-0204585 (PGK), the Special Research Account of the University of Athens (GT, DJF), the Binational (US-

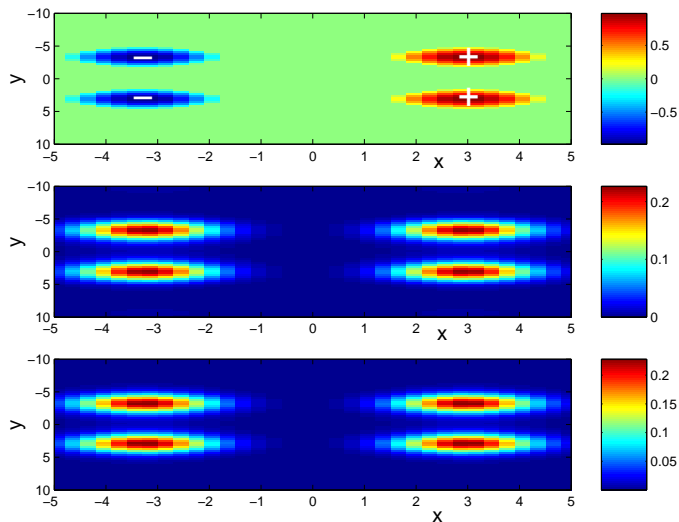


Figure 6. The top panel shows the contour plot of the real part of the initial configuration consisting of two pairs of pulses which are π out of phase (hence the total phase change, as one goes around the configuration is 2π). The pluses indicate (centers of) the “up-pulses”, whereas the minus signs the “down-pulses” of the initial configuration. The middle and bottom panel show the contour plot of the square modulus of the wave function at $t = 100$ and $t = 200$ respectively. In the latter, we have verified that the total phase shift around the pulse quartet is 2π , hence the vortex retains its topological charge. In this case, $V_0 = 2$, $k = 0.5$, $\phi = 0$, and $\Omega = 0$.

Israel) Science Foundation, under grant No. 1999459 (BAM), and San Diego State University Foundation (RCG).

References

- [1] F. Dalfovo, S. Giorgini, L.P. Pitaevskii, and S. Stringari, *Rev. Mod. Phys.* **71**, 463 (1999).
- [2] S. Burger *et al.*, *Phys. Rev. Lett.* **83**, 5198 (1999); J. Denschlag *et al.*, *Science* **287**, 97 (2000); B.P. Anderson *et al.*, *Phys. Rev. Lett.* **86**, 2926 (2001).
- [3] K.E. Strecker *et al.*, *Nature* **417**, 150 (2002); L. Khaykovich *et al.*, *Science* **296**, 1290 (2002).
- [4] M.R. Matthews *et al.*, *Phys. Rev. Lett.* **83**, 2498 (1999); K.W. Madison, *et al.* *Phys. Rev. Lett.* **84**, 806 (2000); S. Inouye *et al.*, *Phys. Rev. Lett.* **87**, 080402 (2001).
- [5] J.R. Abo-Shaer *et al.*, *Science* **292**, 476 (2001); J.R. Abo-Shaer, C. Raman and W. Ketterle, *Phys. Rev. Lett.* **88**, 070409 (2002); P. Engels *et al.*, *Phys. Rev. Lett.* **89**, 100403 (2002).
- [6] K. Staliunas, S. Longhi and G.J. de Valcárcel, *Phys. Rev. Lett.* **89**, 210406 (2002).
- [7] G. Theocharis, D.J. Frantzeskakis, P.G. Kevrekidis, B.A. Malomed and Yu.S. Kivshar, *Phys. Rev. Lett.* **90**, 120403 (2003).
- [8] B.B. Baizakov, B.A. Malomed, and M. Salerno, “Multidimensional solitons in periodic potentials”, submitted to *Europhys. Lett.*
- [9] B.B. Baizakov, V.V. Konotop, and M. Salerno, *J. Phys. B* **35**, 5105 (2002).
- [10] T. Frisch, Y. Pomeau and S. Rica, *Phys. Rev. Lett.* **69**, 1644 (1992).
- [11] T. Winiecki, J.F. McCann and C.S. Adams, *Phys. Rev. Lett.* **82**, 5186 (1999).
- [12] R.J. Donnelly, *Quantized Vortices in He II* (Cambridge University Press, Cambridge 1991).
- [13] S. Inouye *et al.*, *Nature* **392**, 151 (1998); E.A. Donley *et al.*, *Nature* **412**, 295 (2001).
- [14] A.L. Fetter and A.A. Svidzinsky, *J. Phys.: Cond. Matter* **13**, R135 (2001).
- [15] M. Greiner, I. Block, O. Mandel, T.W. Hänsch and T. Esslinger, *Appl. Phys. B* **73**, 769 (2001).
- [16] A. Trombettoni and A. Smerzi, *Phys. Rev. Lett.* **86**, 2353, (2001).

- [17] F.Kh. Abdullaev, B.B. Baizakov, S.A. Darmanyan, V.V. Konotop, and M. Salerno, *Phys. Rev. A* **64**, 043606 (2001).
- [18] A. Smerzi, A. Trombettoni, P.G. Kevrekidis, and A.R. Bishop, *Phys. Rev. Lett.* **89**, 170402 (2002)
- [19] F.S. Cataliotti *et al.*, cond-mat/0207139.
- [20] O. Morsch and E. Arimondo, in *Dynamics and Thermodynamics of Systems with Long-Range Interactions*, T. Dauxois, S. Ruffo, E. Arimondo and M. Wilkens (Eds.), Springer (Berlin 2002), pp. 312-331.
- [21] Y.B. Band, I. Towers, and B.A. Malomed, *Phys. Rev. A* **67**, 023602 (2003).
- [22] P.A. Ruprecht, M.J. Holland, K. Burnett and M. Edwards, *Phys. Rev. A* **51**, 4704 (1995).
- [23] J.J. García-Ripoll and V.M. Pérez-García, cond-mat/001207.
- [24] B. Jackson, J.F. McCann and C.S. Adams, *Phys. Rev. A* **61**, 013604 (1999).
- [25] J.E. Williams and M.J. Holland, *Nature* **401**, 568 (1999).
- [26] B. Sandstede and A. Scheel, *Phys. Rev. Lett.* **86**, 171, (2001).
- [27] J. Tempere and J.T. Devreese, *Physica C* **369**, 28 (2002).
- [28] R. Carretero-González and K. Promislow, *Phys. Rev. A* **66** 033610 (2002).
- [29] R. Carretero-González and K. Promislow, *Breathing behavior of coupled Bose-Einstein condensates: from multi-soliton interactions to homoclinic tangles* (preprint); see: <http://www.rohan.sdsu.edu/~rcarrete/publications/>
- [30] D.J. Frantzeskakis, G. Theocharis, F.K. Diakonov, P. Schmelcher and Yu.S. Kivshar, *Phys. Rev. A* **66** 053608 (2002).
- [31] M. Peyrard and M.D. Kruskal, *Phys. D* **14**, 88-102 (1984).
- [32] Yu.S. Kivshar and B.A. Malomed, *Rev. Mod. Phys.* **61**, 763 (1989).
- [33] P.G. Kevrekidis and M.I. Weinstein, *Phys. D* **142**, 113 (2000).
- [34] D.S. Rokhsar, *Phys. Rev. Lett.* **79**, 2164 (1997).
- [35] P.O. Fedichev and G.V. Shlyapnikov, *Phys. Rev. A* **60**, R1779 (1999).
- [36] G.B. Hess, *Phys. Rev.* **161**, 189 (1967).
- [37] B.A. Malomed, *Physica D* **32**, 393 (1988).
- [38] B.A. Malomed and P.G. Kevrekidis, *Phys. Rev. E* **64**, 026601 (2001).
- [39] P.G. Kevrekidis, B.A. Malomed, and Yu.B. Gaididei, *Phys. Rev. E* **66**, 016609 (2002).
- [40] T. Kapitula, P.G. Kevrekidis and B. Malomed, *Phys. Rev. E* **63**, 036604 (2001).